IEEE Photonics Journal
An IEEE Photonics Society Publication

Open Access

All-Silicon Terahertz Metasurface With Sharp Fano Resonance and Its Sensing Applications

Volume 13, Number 2, April 2021

Yajun Zhong
Lianghui Du
Qiao Liu
Liguo Zhu
Yi Zou
Bin Zhang

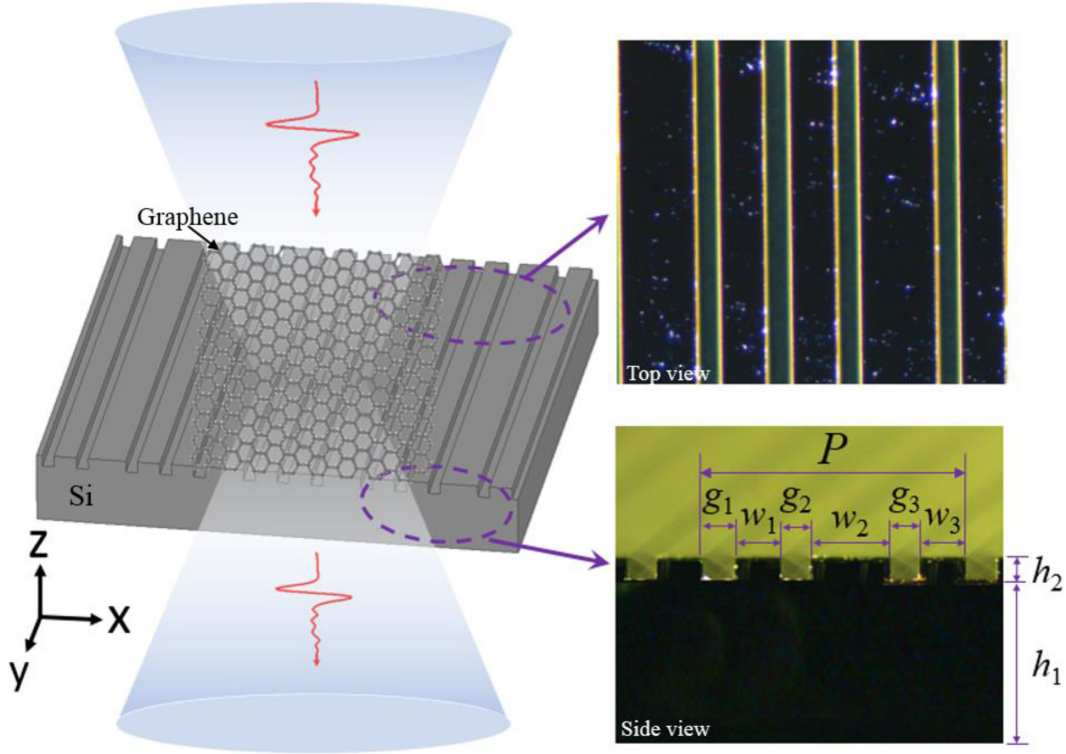

DOI: 10.1109/JPHOT.2021.3065096

All-Silicon Terahertz Metasurface With Sharp Fano Resonance and Its Sensing Applications

Yajun Zhong,[1,2] Lianghui Du,[1,3] Qiao Liu,[1,3] Liguo Zhu,[1,3] Yi Zou,[1] and Bin Zhang[2]

[1]Institute of Fluid Physics, China Academy of Engineering Physics, Mianyang, Sichuan 621900, China
[2]College of Electronics and Information Engineering, Sichuan University, Chengdu, Sichuan 610065, China
[3]Microsystem and Terahertz Research Center, China Academy of Engineering Physics, Mianyang, Sichuan 621900, China

DOI:10.1109/JPHOT.2021.3065096

Manuscript received January 24, 2021; revised February 22, 2021; accepted March 7, 2021. Date of publication March 11, 2021; date of current version March 26, 2021. This work was supported in part by the National Natural Science Foundation of China under Grants U1730246, 11704358, and 81801748, in part by Distinguished Young Scholars of Sichuan Province under Grant 2020JDJQ0008, in part by the Sichuan Science and Technology Program under Grant 2018JY0553, in part by the Major Military Logistics Scientific Research Projects under Grant AWS17J007, in part by the National Key Research and Development Project under Grant 2020YFA0714001, and in part by the Foundation of President of China Academy of Engineering Physics under Grant YZJJLX2018001. Corresponding authors: Lianghui Du; Bin Zhang (e-mail: Lianghui_Du@163.com; zhangbinff@sohu.com).

Abstract: The all silicon terahertz metasurface with sharp Fano resonance and its sensing applications with high Q factor have been investigated. Such metasurface, composed of periodic grooves, can be fabricated by deep silicon etching on high-resistivity silicon. When the refractive index of the sample changes, the shifted resonance frequency appears and the resonance intensity can be modulated by altering the surface conductivity. The Q characteristics of the metasurface and the applications of graphene sensing are then analyzed and verified. The results indicates that the Q factor of the metasurface can reach 39857, the standard sensitivity is 16042 nm/RIU, and the FOM is 533. Meanwhile, the characteristics of sensing graphene samples (∼1 nm) are very useful for sensing other ultra-thin materials or biomolecules.

Index Terms: All-silicon metasurface, sharp resonance, refractive index sensing, graphene sensing.

1. Introduction

Metasurfaces composed of periodic resonant elements have been widely used in terahertz (THz) biosensors, chemical detection, molecular detection, solution sensing and a variety of other applications [1]–[6]. Metasurfaces are very sensitive to slight variation in the surrounding environment [7], [8], because they can enhance the local electric field in a certain frequency band with high Q factor. In practical applications, a higher Q factor usually implies stronger electromagnetic field confinement and higher sensitivity [9], [10]. In order to increase the Q factor, many metasurfaces based on metallic or dielectric structure have been reported in recent years [11]–[14]. Among them, using Fano resonance is an effective method to improve the Q factor and the sensitivity.

However, the Q factors of metal-based resonant systems are limited to $<\sim$10 due to the inevitable non-radiative loss [15]. Therefore, the researchers have designed all-dielectric THz metasurfaces to overcome the ohmic loss of metallic materials and further achieve high Q factor of up to 10000 [16].

The all-dielectric metasurfaces in THz region for different applications have been widely studied [17]–[20]. Tian Ma et al. reported an all-dielectric metamaterial based on the electromagnetically induced transparency (EIT) in terahertz range with Q factor of 75.7, sensitivity of 231 GHz/RIU, and figure of merit (FOM) of 12.7 [21]. Song Han et al. experimentally studied all-dielectric active terahertz photonics driven by bound states in the continuum (BIC) with measured maximum Q factor of 250 [22]. Subhajit Karmakar et al. used stacked metamaterials to achieve refractive index sensing with a sensitivity up to 1 THz/RIU and FOM of around 14.05 [23]. After achieving high Q factor and high sensitivities based on different principles and structures, one of the major challenges for terahertz research is that it is difficult to detect very thin samples, called thin films, using conventional methods [24], so researchers have begun to explore the sensing of ultra-thin samples with the metasurface. The interaction between metasurface and monolayer graphene has been studied in recent years. The interaction between monolayer graphene and metal metasurface with Fano resonance was analyzed theoretically and experimentally in [Ref. 25, which demonstrated that metasurface can detect an analyte that is λ/1000000 thinner than the free space wavelength. Then, Ref. 26 numerically studied the interaction between the metal metasurface and the multilayer graphene. However, the works related to THz sensing by using all-silicon terahertz metasurfaces with sharp Fano resonance, especially the layer number sensing for graphene, have rarely been reported yet. In order to further promote the development of ultra-sensitive metasurface, especially the detection of ultra-thin materials, it is still of great significance and challenge to design the all-dielectric metasurface and study its applications with higher Q factor in THz region.

In this paper, the terahertz all-silicon metasurface with sharp resonance has been designed and its applications in refractive index sensing and graphene sensing have further been investigated. The all-silicon metasurface is composed of periodic grooves that can be obtained by deep silicon etching on the high-resistivity silicon. The structure of the metasurface is not only easy to be processed, but also can achieve Fano resonance with high Q factor. When the analytes with different refractive index are attached to the metasurface, the frequency resonance will be shifted and the resonance intensity will also be modulated due to the change of surface conductivity. The high Q characteristics of metasurface and the applications of graphene sensing have been verified theoretically and experimentally. By optimizing the structure parameter, both ultra-high Q factor and FOM have been achieved, which are beneficial to the applications in refractive index sensing. Meanwhile, the characteristics of sensing ultra-thin samples ($\sim$1 nm) provide a promising approach for sensing in other ultra-thin materials or biomolecules with the high conductivity.

2. Structure Design

The conceptual view of the all-silicon metasurface sensor is illustrated in Fig. 1(a). The metasurface is composed of periodic grooves with different width and spacing etched on the high-resistivity silicon. When the metasurface is irradiated by THz waves with electric field along x axis, the Fano resonance will be excited. Consequently, the THz waves are trapped near the grooves, creating the sharp dips in the transmission curve of the metasurface. When the refractive index of the sample changes, the peak resonance frequency of the metasurface will be shifted and the resonance intensity tends to be modulated for different conductivities of the samples on the metasurface, which can be utilized for ultrasensitive terahertz sensing.

The micrograph and the geometrical parameters of the metasurface are shown in Fig. 1(b) and Fig. 1(c). The side view of the metasurface fabricated by deep silicon etching is consistent with the structure in the simulation model. The periodic unit of the metasurface is composed of three gaps with different spacing widths, and the main parameters affecting the metasurface performance have been marked in Fig. 1(c). In order to analyze the resonance intensity and sensing characteristics of the metasurface accurately, the two-dimensional simulation model has been established by the

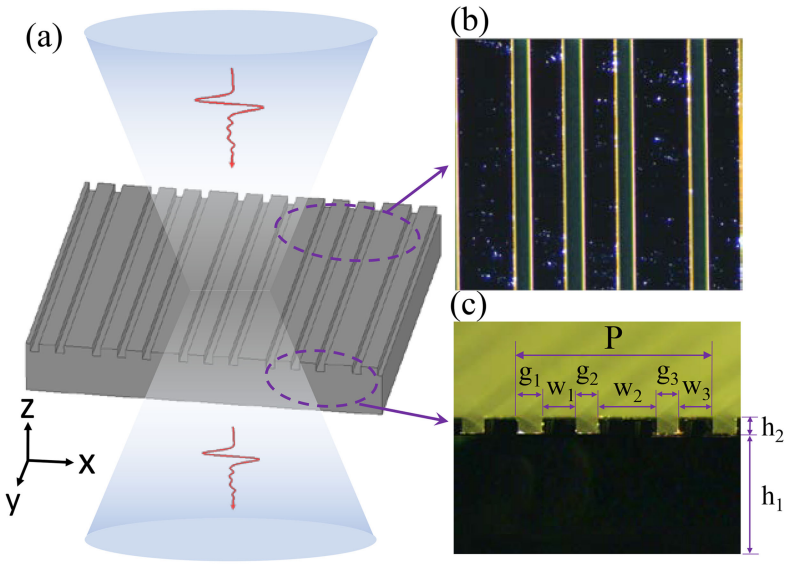

Fig. 1. (a) Conceptual view of the all-silicon metasurface sensor. When the sensor is placed in the transmitted THz-TDS, the change of refractive index and conductivity of the sample on the metasurface can be sensitively perceived by analyzing the transmission curve. (b) The top view of the periodic cell structure, which consists of three gaps with different spacing widths. (c) The side view of the periodic cell structure, annotating the main structure parameters.

use of the electromagnetic simulation software Comsol Multiphysics. In the simulation model, wave optical module is used for modeling, the solver adopts frequency domain stationary, and physics-controlled mesh can be used for mesh setting. The periodic boundary conditions along x axis are employed to the unit cell and perfect matched layers (PMLs) are set at the ends in the z direction. Finally, the structure parameters of the metasurface are set as $w_1 = 95\ \mu$m, $w_2 = 160\ \mu$m, $w_3 = 95\ \mu$m, $g_1 = 55\ \mu$m, $g_2 = 50\ \mu$m, $g_3 = 50\ \mu$m, $h_1 = 450\ \mu$m, $h_2 = 50\ \mu$m.

It is well known that the Fabry-Perot (F-P) resonance will occur for a dielectric slab when the refractive index is high enough [27]. The reflection and transmission curves of terahertz waves passing through high-resistivity silicon with a thickness of 500 μm have been firstly calculated. In the simulation model, the middle part is high-resistivity silicon, the upper and lower layers are vacuum, and the F-P resonance can be clearly found in Fig. 2(a). The corresponding electric field distribution at 0.4436 THz shown in Fig. 2(b) indicates that the F-P resonance arises from the interference of multiple reflections in the two interfaces of the silicon.

When designing the metasurface, it is difficult to excite sharp resonance with symmetrical grooves structure, so it is necessary to design asymmetrical periodic grooves on the surface. When the grooves with different width and spacing are etched on the surface of high-resistivity silicon, the asymmetric periodic structure will form a narrowband dark mode to interfere with the broadband F-P resonance, exciting sharp Fano resonances [27]. For the sake of convenience without loss of generality, the resonance peak at 0.4436 THz within the range of 0.4 THz $\sim$ 0.6 THz is taken as an example, as shown in Fig. 2(c). Fig. 2(d) further shows the electric field distribution at 0.4436 THz, which reveals that the electric field is tightly confined in the grooves and the silicon surface. The weakly scattered electromagnetic field generated by resonance effectively prevents the electric field coupling to the free space, leading to the reduction of the radiation loss, and finally realizing the sharp Fano resonance. The stronger ability to confine the electric field means the higher Q factor of the resonance. When the surface is covered with thin film, the ability of the metasurface to confine the electric field will be weakened, and the electric field intensity in the grooves will be reduced, which provides powerful conditions for the applications of terahertz sensing. Moreover, as the electric field is mainly confined in the grooves, the width of the grooves will affect the distribution

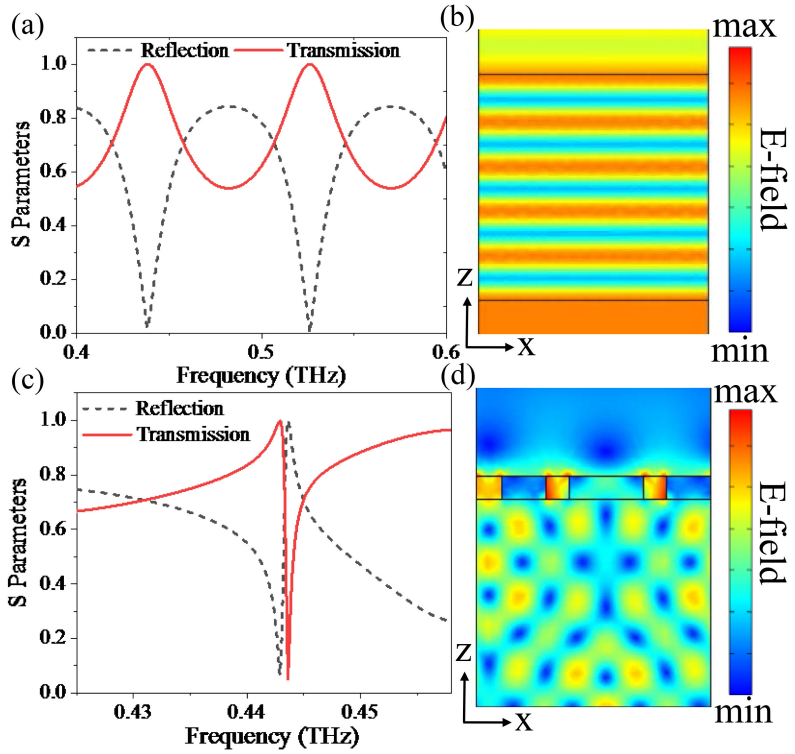

Fig. 2. (a) Reflection and transmission of terahertz waves through high-resistivity silicon with a thickness of 500 μm (b) The electric field distribution of F-P resonance. (c) The reflection and transmission of Fano resonance at 0.4436 THz. (d) The electric field distribution at 0.4436 THz.

of electric field sensitively, which is benefitial for achieving higher Q resonance by optimizing the grooves width.

3. Sensing Performance

In order to analyze the resonance characteristics of the all-silicon metasurface, detailed analysis of the Fano resonance are performed by fitting the transmission spectra using the Fano-formula, as shown in Fig. 3(a). The Fano formula is given by [28]:

$$T_{Fano} = |a_1 + ia_2 + b/(\omega - \omega_0 + i\gamma)|^2 \quad (1)$$

where a_1, a_2 and b are constant real numbers, ω_0 is the Fano resonance frequency, γ is the overall damping rate of the resonance, and the Q factor can be determined as $Q = \omega_0/2\gamma$. According to the linewidth and resonance frequency shown in Fig. 3(a), $\omega_0 = 2\pi * 0.4436$ THz and $Q = 928$.

It is well known that the sharp resonance can be applied as an ultrasensitive sensor for refractive index sensing. Fig. 2(d) indicates that the electric field of the metasurface is confined on the surface, leading to the sensitive shift of the resonance peak for different refractive index on the surface of the metasurface.

According to the simulation results, when the refractive index of the analyte increases from 1.0 to 1.2 in steps of 0.05, the resonant frequency is redshift, as shown in Fig. 3(b). The calculation results show that the sensitivity is 7.5 GHz/refractive index unit (RIU) and the standard sensitivity of resonance is obtained using the formula [29], i.e.,

$$S = \left|\frac{d\lambda}{dn}\right| = \frac{c}{f_0^2} \times \frac{df}{dn} = 11434nm/RIU \quad (2)$$

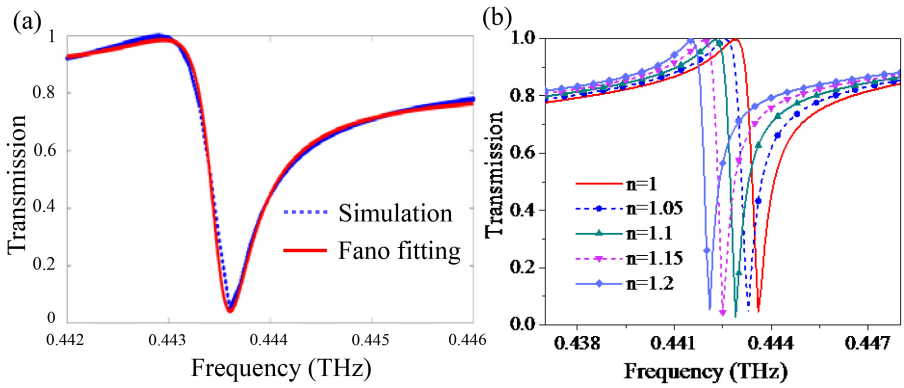

Fig. 3. (a) The Fano lineshape fitting for the transmission. (b) The transmission of the metasurface for different refractive index of analyte ranging from 1 to 1.2 with steps of 0.05.

where c is the speed of light in vacuum, f_0 denotes the resonance frequency, and n represents the refractive index of the analyte. For the sensing application, FOM is usually applied to evaluate the performance of the ultrasensitive sensor. The FOM of this sensor can be calculated using the formula [29], i.e.,

$$FOM = \frac{S}{\Delta\lambda} = \frac{1}{f_0} \times \frac{df}{dn} \times Q = 10.7 \tag{3}$$

Additionally, the resonance variation with and without monolayer graphene covered on the metasurface have been calculated to further analyze the sensing performance, as shown in Fig. 4(a). In the presence of the monolayer graphene, the resonance strength decreases significantly, indicating that the graphene film with a sheet conductivity of 0.35 mS alters the state of surface electric field. The thickness of monolayer graphene film is about 1 nm, which is λ/1000000 smaller than the wavelength of THz waves in free space. It is worth pointing out that the ability to detect an analyte with a thickness of 1 nm is very useful for sensing other ultra-thin materials or biomolecules with the high conductivity [25].

In order to characterize the variation in resonance strength due to the addition of monolayer graphene, the difference between the transmission peaks with and without graphene is defined as $\Delta T = |T_0\text{-}T_g| \times 100\%$, where T_0 and T_g are the transmission amplitudes at the dip of the Fano resonance without and with the graphene layer, respectively, as shown in Fig. 4(a). According to the simulation results, $\Delta T = 43.7\%$, which is higher than17.28% of Ref. [26] and 30% of Ref. [25], which also proves that the sensor sensitivity of this all-silicon metasurface to graphene is better than that of metal metasurface. As the number of graphene layers changes from 1 to 3, the surface conductivity of multilayer graphene is 0.35 mS, 0.8 mS and 1.2 mS, respectively [30]. When the number of graphene layers covered on the surface increases from 1 to 3 in the simulation model, the resonance intensity decreases successively, as shown in Fig. 4(b).

The increase of the conductivity on the metasurface can change the original F-P resonance mode, and further suppress the Fano resonance, resulting in the active modulation of the transmission amplitude. Moreover, it can be seen from the electric field distribution in Fig. 4(c) that when the number of graphene layers increases, the strong radiation is coupled to the free space, which leads to a broader resonance and a lower Q factor. In order to quantitatively compare the variation of resonance strength with the increase of graphene layers, transmission peaks is defined as $\Delta P = P_1\text{-}P_2$, where P_1 and P_2 refer to the maximum and minimum values of the resonance peak, respectively. The calculation results in Fig. 4(d) show that as the number of graphene layers increases from 0 to 3, the Q factor decreases from 928 to 92, and ΔP decreases from 0.95 to 0.05,

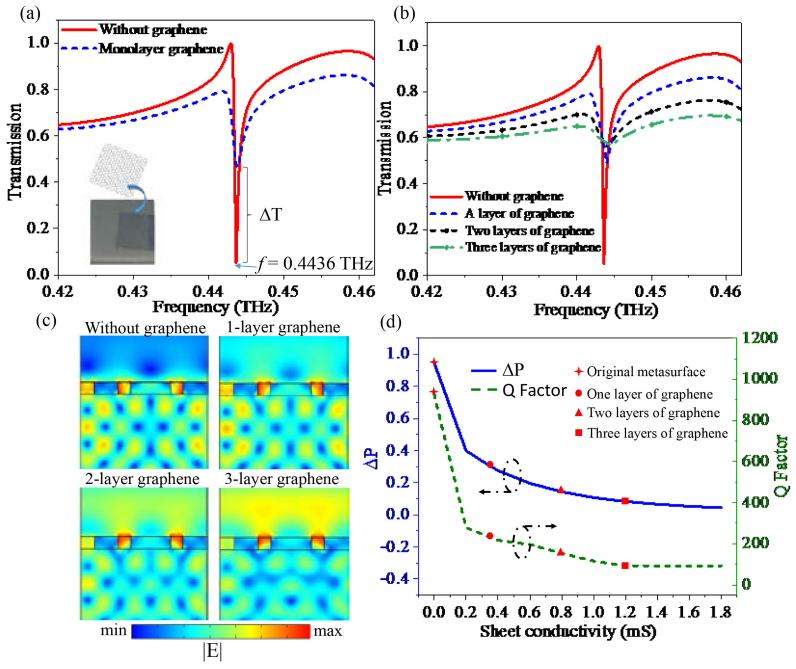

Fig. 4. (a) Transmission spectra of the metasurface with and without the graphene layer. Inset shows a schematic diagram of the transferring monolayer graphene. (b) The transmission spectra of the metasurface with different layers of graphene. (c) The electric field distribution on the metasurface with different graphene layers. (d) The variation of parameters ΔP and Q values with different graphene layers.

which also prove that the increase of graphene layers leads to the increase of radiation loss and the suppression of the Fano resonance.

4. Results and Discussion

In order to verify the sensing characteristics of the all-silicon metasurface sensor, the periodic groove structure has been etched on the high-resistivity silicon with a thickness of 500 μm using the deep silicon etching process. The metasurface samples have been measured by the homemade THz-TDS, which uses a femtosecond fiber laser that emits ultrashort laser pulses with a central wavelength of 1560 nm, an average power of 35 mW and a repetition frequency of 100 MHz to drive a pair of photoconductive antennas for generating and detecting the terahertz pulses. The terahertz waves are focused through the dielectric lens so that the spot diameter at the focal point is about 3 mm.

During the experiment, first of all, the signals of terahertz waves passing through the air have been measured as reference signals, and then the metasurface has been measured. Consequently, the transmission of the metasurface can be calculated. This experimental method can effectively weaken the influence of water in the air on the transmission curve. The F–P resonance effect can be clearly seen in Fig. 5(a), and there is a sharp dip in the transmission curve at 0.4438 THz, which corresponds to the resonance peak at 0.4436 THz in the simulation results. The F-P resonance and Fano resonance can be characterized by the transmission curve in the experimental results, which verifies the validity of theoretical calculation and processing technology. Considering the influence of delay line in the THz-TDS, the scanning time was set at 200 ps and the corresponding spectral resolution is 5 GHz. Therefore, the frequency resolution of 0.1 GHz cannot be arbitrarily set as in the simulation, and the peak of Fano resonance measured in the experiment is not as sharp as

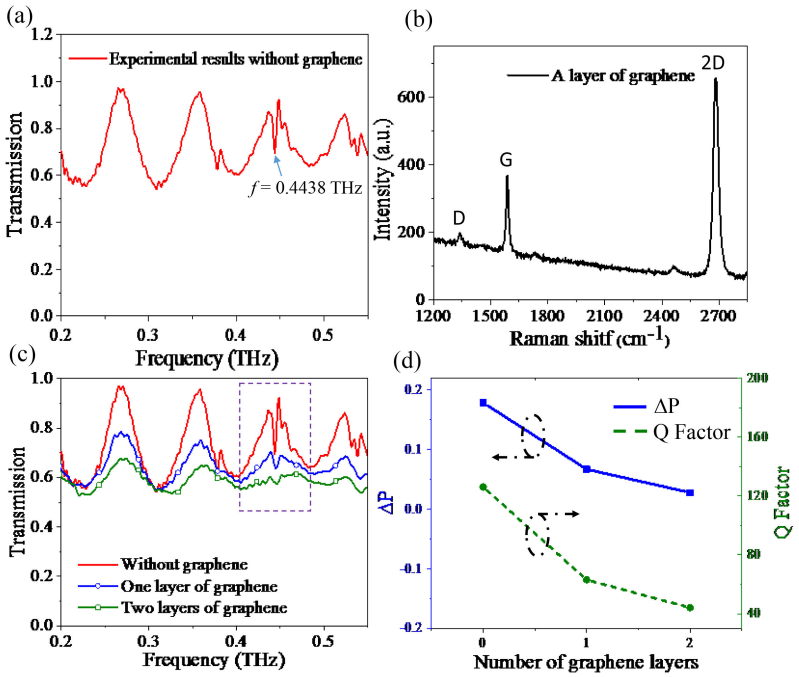

Fig. 5. (a) The transmission of the all-silicon metasurface measured by the homemade THz-TDS. (b) Raman spectra of the monolayer graphene on the quartz substrate; (c) Transmission spectra of the metasurface with and without the graphene layer measured by the homemade THz-TDS. (d) The variation of parameters ΔP and Q factor with different graphene layers based on the experimental results.

that in the simulation due to the limitation of frequency resolution. In order to analyze the influence of fabrication tolerance on the experimental results, the irregular bulge at the bottom of the grooves and the inclined groove walls have also been considered in the simulation. The simulation results show that when the structure changes slightly, the resonance will be affected. Fortunately, the sharp Fano resonance can still be excited. Therefore, the main reason for the decrease of Q factor in the experiment results is the limitation of the system resolution. In addition, it can be seen from the Fig. 5(c) that the transmission of the metasurface decreases with the increase of graphene layers at other frequencies. This is because the increase of graphene layers and the surface conductivity will inevitably lead to the decrease in transmission. Here, we focus on comparing and verifying the variation of the Fano resonance peak at the resonant frequency.

The monolayer graphene film with an area of 1 cm^2 was synthesized by standard chemical vapor deposition (CVD) process. By using a one-step transfer method in purified water, graphene film can be gently transferred onto the quartz substrate, and the Raman spectra were obtained with a 532 nm excitation laser, as shown in Fig. 5(b). The two obvious peaks in the Raman spectra of graphene are the G peak at ∼1591 cm^{-1} and 2D peak at ∼2687 cm^{-1}, and the nearly disappeared D peak demonstrates a high quality of monolayer graphene with very few defects [31].

Next, the sensing performance of the metasurface on graphene can be verified. In the experiment, the transmission of 1-layer and 2-layer graphene on the metasurface have been measured and calculated successively, as shown in Fig. 5(c). According to the calculation methods mentioned above, the Q factor and ΔP at the resonance frequency in the experimental results are shown in Fig. 5(d). It can be seen that the variation trend of Q factor and ΔP with different graphene layers in the experimental results are consistent with that of simulation results. Due to the limitation of the delay line in the THz-TDS, only the variation trend of the resonance peak can be analyzed. According to the experimental results at 0.4438 THz, the Q factor decreases from 126 to 44 as the number of graphene layers increases from 0 to 2, while ΔP decreases from 0.18 to 0.03.

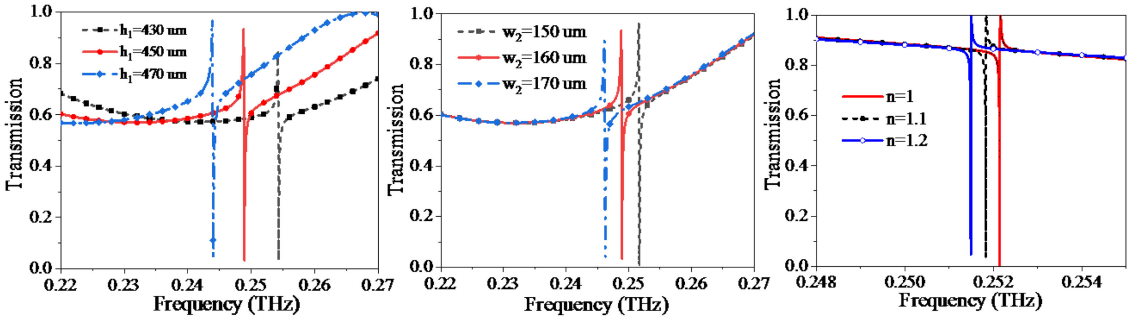

Fig. 6. (a) The variation of the Fano resonance of the metasurface with different thickness substrates. (b) The variation of the Fano resonance of the metasurface with different grooves spacing. (c) The transmission of the metasurface with high *Q* factor for different refractive index of analyte ranging from 1 to 1.2 with steps of 0.1.

Table 1
Comparison of Q Factor and FOM for Various Sensors in THz Range

	Our work	Ref. [32]	Ref. [33]	Ref. [34]	Ref. [21]	Ref. [16]	Ref. [35]
Q factor	39587	19.2	98.33	60	75.7	10800	3189
FOM	553	3.64	101.67	20	12.7	< 20	515

The all-silicon Metasurface with sharp Fano resonance has been verified theoretically and experimentally, and it can be applied to refractive index sensing and graphene sensing. In fact, the metasurface sensor can achieve higher Q factor by optimizing and selecting resonances in different frequency bands.

Since the resonance with high Q factor is excited through periodic groove structure interference F-P resonance, the frequency of resonance peak will be shifted by changing the thickness of the substrate. When the substrate thickness h_1 increases, the resonance frequency will be red shifted, and the calculation results are shown in Fig. 6(a). In the periodic structure, the spacing width of the gap is w_1, w_2 and w_3, respectively. When the spacing width w_2 increases, the resonance frequency will also be red shifted significantly, as shown in Fig. 6(b). Therefore, the resonance frequency can be adjusted arbitrarily by modifying the structure parameters.

By optimizing the structure parameters, the ultra-high Q factor metasurface sensor can be achieved, and the geometric parameters are $w_1 = 95\ \mu$m, $w_2 = 105\ \mu$m, $w_3 = 95\ \mu$m, $g_1 = 35\ \mu$m, $g_2 = 30\ \mu$m, $g_3 = 30\ \mu$m, $h_1 = 350\ \mu$m, $h_2 = 50\ \mu$m. The transmission of the metasurface with ultra-high Q factor for different refractive index of analyte ranging from 1 to 1.2 with steps of 0.1 have been calculated and shown in Fig. 6(c). Using the fitting method mentioned above, $Q = \omega_0/2\gamma = 39587$ can be obtained. Additionally, the standard sensitivities of resonances $S = 16042$ nm/RIU, FOM = 533. Next, the sensor performance of the all-silicon metasurface sensor designed in this paper is quantitatively compared with other terahertz metasurface sensors. Among them, Q factor and FOM are mainly compared, as shown in Table 1.

Typical metasurface sensors in the THz range based on different structures and principles are listed in the table. To the best of our knowledge, the Q factor and FOM of the all-silicon metasurface designed in this paper are much larger than the previously reported results based on the metal resonance structures [32], [33] and dielectric structures [16], [21], [35] in THz range.

5. Conclusion

In summary, the terahertz all-silicon metasurface with sharp resonance and its sensing applications have been investigated. The metasurface is composed of periodic grooves and can be fabricated by deep silicon etching on the high-resistivity silicon with a thickness of 500 μm. When different refractive index samples are attached to the metasurface, the shifted resonance frequency appears and the resonance intensity can be modulated by altering the surface conductivity. The resonance characteristics and the applications of graphene sensing of the metasurface with Q factor of 928 have been verified. In addition, the resonance frequency and the Q factor can be adjusted by modifying the structure parameters and selecting resonances in different frequency bands. By optimizing the structure parameters, the Q factor can reach 39587, the standard sensitivity of resonances is 16042 nm/RIU, and the FOM is 533, which has significant advantages in the application of refractive index sensing. Meanwhile, the characteristics of sensing graphene samples ($\sim$1 nm) are very useful for sensing other ultra-thin films or biomolecules in THz range.

References

[1] H. Tao *et al*., "Metamaterials on paper as a sensing platform," *Adv. Mater.*, vol. 23, no. 28, pp. 3197–3201, 2011.
[2] H. R. Park, K. J. Ahn, S. Han, Y. M. Bahk, N. Park, and D. S. Kim, "Colossal absorption of molecules inside single terahertz nanoantennas," *Nano Lett.*, vol. 13, no. 4, pp. 1782–1786, 2013.
[3] C. Zhang *et al*., "Label-free measurements on cell apoptosis using a terahertz metamaterial-based biosensor," *Appl. Phys. Lett.*, vol. 108, no. 24, pp. 209–233, 2016.
[4] X. Wu, X. Pan, B. Quan, X. Xu, C. Gu, and L. Wang, "Self-referenced sensing based on terahertz metamaterial for aqueous solutions," *Appl. Phys. Lett.*, vol. 102, no. 15, 2013, Art. no. 151109.
[5] X. Hu *et al*., "Metamaterial absorber integrated microfluidic terahertz sensors," *Laser Photon. Rev.*, vol. 10, no. 6, pp. 962–969, 2016.
[6] B. You, C. Y. Chen, C. P. Yu, T. A. Liu, T. Hattori, and J. Y. Lu, "Terahertz artificial material based on integrated metal-rod-array for phase sensitive fluid detection," *Opt. Exp.*, vol. 25, no. 8, pp. 8571–8583, 2017.
[7] M. Seo and H. R. Park, "Terahertz biochemical molecule-specific sensors," *Adv. Opt. Mater.*, vol. 8, no. 3, 2019, Art. no. 1900662.
[8] D. O. Ignatyeva *et al*., "All-dielectric magnetic metasurface for advanced light control in dual polarizations combined with high-Q resonances," *Nat. Commun.*, vol. 11, no. 1, 2020, Art. no. 5487.
[9] S. Karmakar, S. Banerjee, D. Kumar, G. Kamble, R. K. Varshney, and D. R. Chowdhury, "Deep-Subwavelength coupling-induced fano resonances in symmetric terahertz metamaterials," *Phys. Status Solidi-R.*, vol. 13, no. 10, 2019, Art. no. 1900310.
[10] S. Karmakar, D. Kumar, R. K. Varshney, and D. R. Chowdhury, "Lattice-induced plasmon hybridization in metamaterials," *Opt. Lett.*, vol. 45, no. 13, pp. 3386–3389, 2020.
[11] L. Yao *et al*., "Bound states in the continuum in anisotropic plasmonic metasurfaces," *Nano Lett.*, vol. 20, no. 9, pp. 6351−6356, 2020.
[12] W. Xu, L. Xie, and Y. Ying, "Mechanisms and applications of terahertz metamaterial sensing: A review," *Nanoscale*, vol. 9, no. 37, pp. 13864–13878 2017.
[13] Z. J. Liu *et al*., "High-Q quasibound states in the continuum for nonlinear metasurfaces," *Phys. Rev. Lett.*, vol. 123, no. 25, 2019, Art. no. 253901.
[14] L. Liu *et al*., "High-Q hybridized resonance in a plasmonic metasurface of asymmetric aligned magnetic dipoles," *Appl. Phys. Lett.*, vol. 117, no. 8, 2020, Art. no. 081108.
[15] Y. Yang, I. I. Kravchenko, D. P. Briggs, and J. Valentine, "All-dielectric metasurface analogue of electromagnetically induced transparency," *Nat. Commun.*, vol. 5, 2014, Art. no. 5753.
[16] K. Okamoto, K. Tsuruda, S. Diebold, S. Hisatake, M. Fujita, and T. Nagatsuma. "Terahertz sensor using photonic crystal cavity and resonant tunneling diodes," *J. Infrared Millim. Te. Waves*, vol. 38, no. 9, pp. 1085–1097, 2017.
[17] K. Bi *et al*., "Experimental demonstration of ultra-large-scale terahertz all-dielectric metamaterials," *Photon. Res.*, vol. 7, no. 4, pp. 457–463, 2019.
[18] Q. S. Wei *et al*., "Simultaneous spectral and spatial modulation for color printing and holography using all-dielectric metasurfaces," *Nano Lett.*, vol. 19, no. 12, pp. 8964–8971, 2019.
[19] C. Lan, D. Zhu, J. Gao, B. Li, and Z. Gao, "Flexible and tunable terahertz all-dielectric metasurface composed of ceramic spheres embedded in ferroelectric/elastomer composite," *Opt. Express*, vol. 26, no. 15, pp. 19043–19043, 2018.
[20] M. A. Cole, D. A. Powell, and I. V. Shadrivov, "Strong terahertz absorption in all-dielectric huygens' metasurfaces," *Nanotechnology*, vol. 27, no. 42, 2016, Art. no. 424003.
[21] T. Ma, Q. Huang, H. He, Y. Zhao, X. Lin, and Y. Lu, "All-dielectric metamaterial analogue of electromagnetically induced transparency and its sensing application in terahertz range," *Opt. Exp.*, vol. 27, no. 12, pp. 16624–16634, 2019.
[22] S. Han *et al*., "All-Dielectric active terahertz photonics driven by bound states in the continuum," *Adv. Mater.*, vol. 31, no. 37, 2019, Art. no. 1901921.
[23] S. Karmakar, D. Kumar, R. K. Varshney, and D. R. Chowdhury, "Strong terahertz matter interaction induced ultrasensitive sensing in fano cavity based stacked metamaterials," *J. Phys. D Appl. Phys.*, vol. 53, no. 41, 2020, Art. no. 415101.

[24] I. Jáuregui-López, P. Rodríguez-Ulibarri, A. Urrutia, S. A. Kuznetsov, and M. Beruete, "Labyrinth metasurface absorber for ultra-high-sensitivity terahertz thin film sensing," *Phys. Status Solidi-R.*, vol. 12, no. 10, 2018, Art. no. 1800375.
[25] Q. Li *et al.*, "The monolayer graphene sensing enabled by the strong Fano-resonant metasurface," *Nanoscale*, vol. 8, no. 39, pp. 17278–17284, 2016.
[26] S. Xiao *et al.*, "Strong interaction between graphene layer and fano resonance in terahertz metamaterials," *J. Phys. D Appl. Phys.*, vol. 50, no. 19, 2017, Art. no. 195101.
[27] M. Song *et al.*, "Sharp fano resonance induced by a single layer of nanorods with perturbed periodicit," *Opt. Exp.*, vol. 23, no. 3, pp. 2895–2903, 2015.
[28] Y. K. Srivastava *et al.*, "Ultrahigh-Q fano resonances in terahertz metasurfaces: Strong influence of metallic conductivity at extremely low asymmetry," *Adv. Opt. Mater.*, vol. 4, no. 3, pp. 457–463, 2016.
[29] A. A. Yanik *et al.*, "Seeing protein monolayers with naked eye through plasmonic fano resonances," in *Proc. Nat. Acad. Sci.*, vol. 108, no. 29, pp. 11784–11789, 2011.
[30] Y. Zhou *et al.*, "Terahertz wave reflection impedance matching properties of graphene layers at oblique incidence," *Carbon*, vol. 96, pp. 1129–1137, 2016.
[31] A. C. Ferrari *et al.*, "Raman spectrum of graphene and graphene layers," *Phys. Rev. Lett.*, vol. 97, no. 18, 2006, Art. no. 187401.
[32] P. R. Tang *et al.*, "Ultrasensitive specific terahertz sensor based on tunable plasmon induced transparency of a graphene micro-ribbon array structure," *Opt. Exp.*, vol. 26, no. 23, pp. 30655–30666, 2018.
[33] X. Qin, G. Dong, B. Wang, and W. Huang, "Design of quad-band terahertz metamaterial absorber using a perforated rectangular resonator for sensing applications," *Nanoscale Res. Lett.*, vol.vol. 13, no. 1, pp. 1–8, 2018.
[34] X. He, F. Lin, F. Liu, and W. Shi, "Tunable high Q-factor terahertz complementary graphene metamaterial," *Nanotechnology*, vol. 29, no. 48, pp. 485205–485216, 2018.
[35] X. Chen and W. Fan, "Ultrahigh-Q toroidal dipole resonance in all-dielectric metamaterials for terahertz sensing," *Opt. Lett.*, vol. 44, no. 23, pp. 5876–5879, 2019.